

Whole-exome sequencing identified genes known to be responsible for retinitis pigmentosa in 28 Chinese families

Chang Shen,^{1,2} Bing You,² Yu-Ning Chen,² Yang Li,² Wei Li,³ Wen-Bin Wei²

¹Department of Ophthalmology, First Affiliated Hospital, College of Medicine, Zhejiang University, Hangzhou, Zhejiang 310003, China; ²Clinical Research Center, First Affiliated Hospital, College of Medicine, Zhejiang University, Hangzhou, Zhejiang, China.; ³Tongren Eye Center, Beijing key Laboratory of Intraocular Tumor Diagnosis and Treatment, Beijing Ophthalmology & Visual Sciences Key Lab, Medical Artificial Intelligence Research and Verification Key Laboratory of the Ministry of Industry and Information Technology, Beijing Tongren Hospital, Capital Medical University, Beijing, China; ³State Key Laboratory of Stem Cell and Reproductive Biology, Institute of Zoology, Chinese Academy of Sciences, Beijing 100101, China; University of Chinese Academy of Sciences, Beijing, China

Purpose: Retinitis pigmentosa (RP) is a group of highly heterogenous inherited retinal degeneration diseases. Molecular genetic diagnosis of RP is quite challenging because of the complicated disease-causing mutation spectrum. The aim of this study was to explore the mutation spectrum in Chinese RP patients using next-generation sequencing technology and to explore the genotype–phenotype relationship.

Method: In this study, a cost-effective strategy using whole-exome sequencing (WES) was employed to address the genetic diagnosis of 28 RP families in China. One to two patients and zero to two healthy relatives were sequenced in each family. All mutations in WES data that passed through the filtering procedure were searched in relation to 662 gene defects that can cause vision-associated phenotypes (including 89 RP genes in the RetNet Database). All patients visiting the outpatient department received comprehensive ophthalmic examinations.

Result: Twenty-five putative pathogenic mutations of 12 genes were detected by WES and were all confirmed by Sanger sequencing in 20 (20/28, 71.4%) families, including the 12 following genes: *USH2A*, *CYP4V2*, *PRPF31*, *RHO*, *RPI1*, *CNGA1*, *CNGB1*, *EYS*, *PRPF3*, *RP2*, *RPGR*, and *TOPORS*. Three families were re-diagnosed as having Bietti crystalline dystrophy (BCD). *USH2A* (4/20, 20%) and *CYP4V2* (3/20, 15%) were found to be the most frequent mutated genes. Seven novel mutations were identified in this research, including mutations in *USH2A1*, *USH2A2*, *PRPF31*, *RP2*, *TOPORS*, *CNGB1*, and *RPGR*. Phenotype and genotype relationships in the 12 RP genes were analyzed, which revealed later disease onset and more severe visual function defects in *CYP4V2*.

Conclusion: Twenty-five putative pathogenic mutations of 12 genes were detected by WES, and these were all confirmed by Sanger sequencing in 20 (20/28, 71.4%) families, including seven novel mutations. *USH2A* and *CYP4V2* were found to be the most frequent genes in this research. Phenotype and genotype relationships were revealed, and the mutation spectrum of RP in Chinese populations was expanded in this research, which may benefit future cutting-edge therapies.

Retinitis pigmentosa (RP) is a group of inherited retinal degeneration diseases that affect retinal photoreceptor cells and RPE cells. With the slow degeneration of rod cells followed by loss of cone cells, patients suffer from progressive visual field constriction and gradual or rapid vision loss until visual acuity is severely affected in their 50s to 60s; some specific types may bring about severe vision loss in early decades. The prevalence of RP worldwide was reported

to be approximately 1/4,000 [1], with a prevalence of 1:1,000 to 1:4,016 in China [2-4].

RP has varied inherited patterns, including autosomal dominant (30%–40%), autosomal recessive (50%–60%), and X-linked (5%–15%) [5]. It shows great genetic heterogeneity, and to date, there have been 89 genes reported to relate to RP in the RetNet Database. The gene spectrum of RP was reported to overlap with other inherited retinal dystrophies (IRDs), including Leber congenital amaurosis (LCA), cone-rod dystrophy (CRD), macular dystrophies, and congenital stationary night blindness (CSNB) [6].

The complicated gene spectrum and inherited pattern of RP raises great challenges to doctors and researchers for genetic diagnosis. With the increasing number of gene therapy approaches in IRDs (e.g., RPE65-associated retinal

Correspondence to: Wen-Bin Wei, Tongren Eye Center, Beijing Key Laboratory of Intraocular Tumor Diagnosis and Treatment, Beijing Ophthalmology & Visual Sciences Key Lab, Medical Artificial Intelligence Research and Verification Key Laboratory of the Ministry of Industry and Information Technology, Beijing Tongren Hospital, Capital Medical University, Beijing 100730, China; Phone: 010-58265736, FAX: 010-58265736; email: weibenbintr@163.com

dystrophies [RDs]-Luxturna [7], *MERTK*-associated RDs [8], and *REPI*-associated RDs [9]), genetic diagnosis was not only beneficial in confirming the diagnosis, predicting disease prognosis, and providing genetic consultant advice, but it was also crucial in identifying patients who could benefit from these emerging novel therapeutic techniques. With the development of next-generation sequencing (NGS), whole-exome sequencing (WES) and panel-based NGS have been widely used in molecular genetic diagnosis of IRDs [10]. Whole-genome sequencing (WGS), which is based on non-PCR technology, can provide more information about the whole genome, including introns and areas that cannot be sequenced using WES and panel-based NGS, such as large indels and copy number variants. However, WGS is much more expensive at this stage than other methods, and it is more complicated in terms of data processing, making it inapplicable for small laboratories [11]. WES, which targets the complete protein coding region in the genome, has been reported to be successful in identifying genetic defects in 60%–80% of Mendelian diseases [12]. Compared with panel-based NGS, which comprises a well-established panel including certain genes, WES can be used to detect novel mutations in IRD patients. The decreasing cost makes it more practical to apply than other NGS approaches are.

In this study, we investigated the disease-causing genes of 28 Chinese families with a clear family history of RP through WES. The results may benefit the RP gene diagnosis and the pathogenic and genotype-phenotype study of RP.

METHODS

Ethics statement: All procedures performed in studies involving human participants were conducted in accordance with the ethical standards of the institutional or national research committee and with the 1964 Declaration of Helsinki and its later amendments or comparable ethical standards. The study was approved by the Medical Ethics Committee of Beijing Tongren Hospital, and written informed consent was obtained from all study participants. All methods were performed in accordance with the relevant guidelines and regulations.

Study subjects: Twenty-eight families with a definite diagnosis of RP and clear family history were recruited from the Beijing Tongren Eye Center from January 2019 to October 2019. The clinical diagnosis of RP was confirmed by an experienced retinal specialist (Dr. Wei Wenbin) with the following diagnostic criteria: 1) typical history and fundus appearance; 2) presence or absence of a family history of night blindness or low vision; 3) defective static perimetry; and 4) defective electroretinogram (ERG). The criteria for defining RP in

the families were based on the probands' and their family members' descriptions, such as poor vision and night blindness, and then confirmed by clinical examinations.

All patients visiting the outpatient department received comprehensive ophthalmic examinations including best-corrected visual acuity (BCVA), intraocular pressure (IOP) measurement (noncontact tonometer, Cannon, Tokyo, Japan), slit-lamp biomicroscopy, color fundus photography (TRC RETINAL CAMERA 50 DX, Topcon Inc., Tokyo, Japan), ocular biometry applying optical low-coherence reflectometry (Lenstar 900 Optical Biometer, Haag-Streit, Koeniz, Switzerland), OCT and OCT angiography (VG200, SVision Imaging, Ltd., Luoyang, China), stationary perimetry tests (Humphery field analyzer; Carl Zeiss Meditec, Inc., Dublin, CA), and ERGs.

WES experiments and data analysis: DNA samples were extracted from whole blood using a DNeasy Blood & Tissue Kit (50; Qiagen, Berlin, Germany) following the manufacturer's instructions. The purity of DNA was determined using a NanoPhotometer® (Implen, San Diego, CA). The concentration of DNA was determined by Qubit® 3.0 Fluorometer (Life Technologies, San Diego, CA).

Whole-exome capture of 83 individuals from 28 RP families (including 55 RP patients and 28 of their healthy relatives) was performed using Agilent SureSelect Human All Exon V6 kits. Then, sequencing was conducted on an Illumina HiSeq X Ten System from Annoroad Gene Tech. Co., Ltd. The sequencing reads were mapped against UCSC hg19 by BWA. Individual sample single-nucleotide polymorphisms (SNPs) and insertion or deletion events (indels) were detected by SAMTOOLS. After generating initial single nonsynonymous variant (SNV) calls, we performed further filtering to identify high-confidence variants that had the following characteristics: (i) they had a quality >Q30 and a depth of $\geq 5\times$, and (ii) they were not located in the major histocompatibility complex homologous sequence. WES data from 1000 Genomes, dbSNP147, the ExAC database, and unrelated healthy individuals from the Annoroad Healthy person mutation database were used as reference data for variant filtering. Prediction of potential functional consequences of variants was conducted using SIFT and PROVEAN [13] and Polymorphism Phenotyping v2 (PolyPhen-2) [14].

The mutations were filtered with the following multiple-step bioinformatics analysis: (1) the SNPs and short indels in the exome region were filtered against data from 1000 Genomes, dbSNP147, ExAC and unrelated individuals of 2020 in-house non-RP controls, removing minor allele frequency (MAF) values that were greater than 0.005 for the recessive model and were greater than 0.001 for the dominant

model; (2) noncoding variants were excluded without altering splicing sites; (3) synonymous variants without were excluded the altering splicing sites in the genes; and (4) missense variants predicted to be Neutral/Tolerated/Benign by PROVEAN, SIFT, and PolyPhen-2 simultaneously were excluded. All mutations that passed through the filtering procedure were searched in a set of 662 gene defects that can cause vision-associated phenotypes (including 89 RP genes in RetNet Database; Appendix 1). Autosomal recessive, autosomal dominant, X-linked, and digenic heredity patterns were included in this research. The pathogenicity of the selected mutations was predicted according to American College of Medical Genetics and Genomics standards and guidelines [15].

PCR and direct Sanger sequencing for variant confirmation: Sanger sequencing was used to validate the pathogenic mutations among patients. Segregation tests were also performed in all the available family members. Primers were designed (Primer Premier 5) to use PCR amplification on the 400–500 bp region flanking the mutation. To ensure high-quality Sanger sequencing, the amplification was designed to have a boundary at least 150 bp away from the mutation base. The amplification was then Sanger sequenced on an Applied BioSystems 3730xl DNA Analyzer (Waltham, MA). The Sanger sequencing results were analyzed with Applied Biosystems' Sequencer software. Compound heterozygous variants were defined as a variant that detected the patient's father and mother, each carrying a heterozygous mutation, or the direct relatives without RP only carrying a heterozygous mutation. Variants were excluded when exactly the same variants were detected in a relative who was not diagnosed with the RP phenotype. When RP patients' mutations were not detected in their biological parents, we defined these mutations as "de novo." Variants were defined as "novel" if they had not been reported in the literature or registered in the HGMD and OMIM databases.

Statistical analysis: All analyses were conducted using SPSS (IBM SPSS for Windows, version 23) and GraphPad PRISM version 8.0 (GraphPad Software Inc.) statistical software. Descriptions of the quantitative data are presented as the means (standard deviations, SDs) and median. Disease durations were calculated as current age minus disease onset age. Disease onset age of patients who could not remember accurately and described the disease onset as early childhood were defined as 5 years old in the calculation.

RESULTS

Twenty-eight Chinese families with a diagnosis of RP were recruited for this study. Of these, 9 were autosomal dominant RP (adRP) families, 17 were autosomal recessive RP (arRP) families, and 2 were X-linked RP families. WES was performed in 83 individuals from 28 RP families (including 55 RP patients and 28 of their healthy relatives), with 2 patients and 0–2 healthy relatives sequenced in each family. All individuals who were sequenced are highlighted with genotype in Figure 1. WES achieved an average of 116.75×depth and an average of 99.88% coverage rate of the exome targeted region. The mapping rate and coverage of the targeted region of each sample are shown in Appendix 2. Sanger sequencing results of each family are listed in Appendix 3.

For 28 RP families, putative pathogenic mutations of 20 (71.4%) families were identified, including the 12 following RP genes (Table 1) [16-31]: *USH2A* (4/20, 20%), *CYP4V2* (3/20, 15%), *PRPF31* (2/20, 10%), *RHO* (2/20, 10%), *RPI* (2/20, 10%), *CNGA1* (1/20, 5%), *CNGB1* (1/20, 5%), *EYS* (1/20, 5%), *PRPF3* (1/20, 5%), *RP2* (1/20, 5%), *RPGR* (1/20, 5%), and *TOPORS* (1/20, 5%). Three families with *CYP4V2* mutations were rediagnosed as having Bietti crystalline dystrophy (BCD). The pedigree charts of the 20 families are listed in Figure 1. All the putative genes cosegregated with the phenotype in RP families. All suspicious mutations found in each family and the reason we chose putative mutations were illustrated in Appendix 4. Putative genes of 7 (7/9, 77.78%) autosomal dominant families, 11 (11/17, 64.71%) autosomal recessive families, and 2 (2/2, 100%) X-linked families were identified. In total, 28 mutations were identified, including 10 (35.17%) missense mutations, 9 (32.14%) frameshift mutations, 5 (17.86%) missplicing mutations, and 4 (14.27%) truncation mutations. The mutation type spectrum of each gene is listed in Appendix 5. The following seven novel mutations were identified in this research: *USH2A*, c.9337dupA(p.I3113fs); *USH2A*, c.C10498T(p.Q3500*); *PRPF31*, c.967_968delGA (E323Dfs*151); *RP2*, c.758_761delTAAT (p.L253fs*10); *TOPORS*, c.2323_2324delAG (p.S775*); *CNGB1*, c.G2006A (p.W669*); *RPGR*, c.T773C (p.L258P).

From the 20 families with confirmed molecular diagnoses, 33 patients visited our outpatient department. Their clinical characteristics are listed in Table 2. The mean age of all patients was 42.9 ± 14.5 years, whereas the mean age of disease onset and mean age of visual acuity decline were 11.7 ± 9.9 years and 33 ± 9.5 years. Of the 33 patients, 26 (78.8%) had an eye with BCVA lower than 0.3, whereas 20 (60.6%) had an eye with BCVA lower than 0.1. The long duration from disease onset to molecular diagnosis and poor preserved

BCVA in this research indicated a late molecular diagnosis in Chinese RP patients.

Phenotype–genotype was detected in this research. Average disease duration, average visual acuity, and average disease onset age were calculated and analyzed as shown in Figure 2. Genes on the left side of the image were found to have a more severe phenotype with shorter disease duration and poor visual acuity; genes on the right side were found to have a milder phenotype. *USH2A* was found to have a disease onset from adolescence, but the visual function exhibited moderate defect over 35 years of disease duration. In contrast, *CYP4V2* was found to have a later disease onset from the 30s, but severe visual function defects were observed in the later 17 years.

In all 12 identified RP genes, four families (20%)—RP008, RP015, RP028, and RP033—were detected to have compound heterozygous mutations in *USH2A* (Table 1), with six mutations. Among all mutations detected, two novel mutations were found—namely, c.C10498T (p.Q3500*) in RP015 and c.9337dupA (p.I3113Nfs*17) in RP033. These two mutations were located in the extracellular matrix protein-related regions, making the subsequent extracellular structure of more than 2,000 amino acids untranslatable, which may have led to damaging effect for Usherin protein [31]. They were identified as pathogenic mutations according to the ACMG guidelines. Patients in all four families were siblings who exhibited the arRP inheritance pattern. Since not all mutations were novel, some of them has been reported previously. The clinical data of the patients in the four families are listed in Table 2. All patients visiting the outpatient

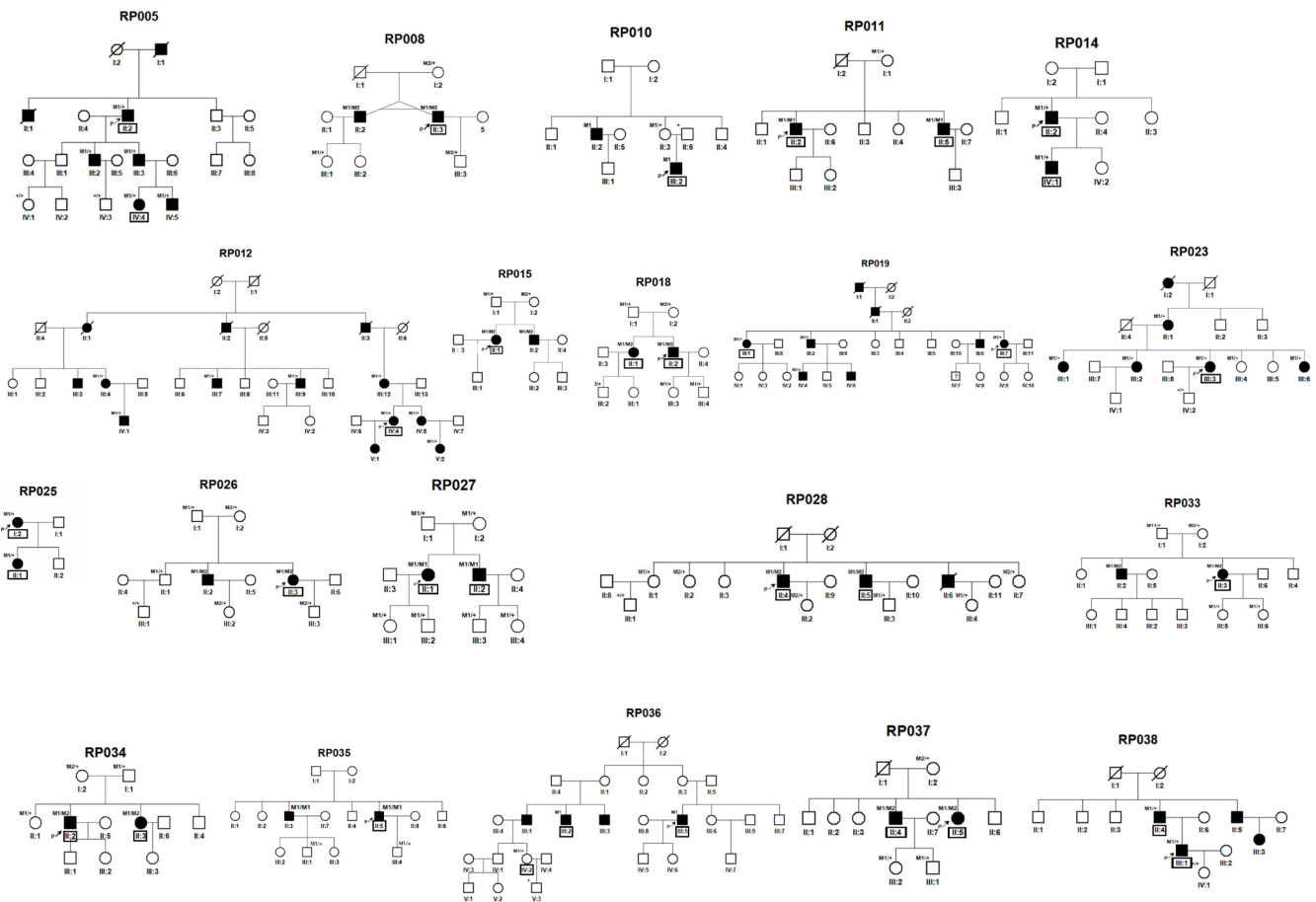


Figure 1. Pedigree charts of the 20 retinitis pigmentosa (RP) families with confirmed molecular diagnosis. The genotype of each individual sequenced is mentioned in bold, and individuals who were clinically investigated in our outpatient department are indicated with black frames.

TABLE 1. PUTATIVE PATHOGENIC MUTATIONS OF KNOWN RP GENES DETECTED IN THE 20 RP FAMILIES.

Family No.	Inheritance Model	Gene	NM No.	Mutation No.	Nucleotide change	Amino acid change	State	Frequencies			Software predictions			Reference
								1000G	ExAC	SIFT	Poly-Phen	PROVEAN		
RP008	AR	USH2A	NM_206933	M1	c.99_100insT	p.R34Sfs*41	comhet	None	None	NA	NA	NA	[16]	
	AR	USH2A	NM_206933	M2	c.8559-2A>G	mis-splicing	comhet	0.000199681	0.00002473	NA	NA	NA	[16]	
RP015	AR	USH2A	NM_206933	M1	c.8559-2A>G	mis-splicing	comhet	0.000199681	<0.000001	NA	NA	NA	[16]	
	AR	USH2A	NM_206933	M2	c.9337dupA	p.I3113Nfs*17	comhet	None	None	NA	NA	NA	N ^o t reported	
RP028	AR	USH2A	NM_206933	M1	c.8559-2A>G	mis-splicing	comhet	0.000199681	0.00002473	NA	NA	NA	[16]	
	AR	USH2A	NM_206933	M2	c.G14287C	p.G4763R	comhet	None	None	D	D	D	[17]	
RP033	AR	USH2A	NM_206933	M1	c.C10498T	p.Q3500*	comhet	None	None	NA	NA	NA	N ^o t reported	
	AR	USH2A	NM_206933	M2	c.T2802G	p.C934W	comhet	0.000798722	0.0002	D	D	D	[18]	
RP026	AR	CYP4V2	NM_207352	M1	c.T219A	p.F73L	comhet	None	0.000008258	T	B	D	[19]	
	AR	CYP4V2	NM_207352	M2	c.G1169A	p.R390H	comhet	None	None	D	D	D	[20]	
RP034	AR	CYP4V2	NM_207352	M1	c.1091-2A>G	mis-splicing	comhet	None	0.00003295	NA	NA	NA	[21]	
	AR	CYP4V2	NM_207352	M2	c.G1199A	p.R400H	comhet	0.000199681	0.00004118	D	D	D	[22]	
RP037	AR	CYP4V2	NM_207352	M1	c.802del17bpinsGC	frameshift	comhet	None	None	NA	NA	NA	[21]	
	AR	CYP4V2	NM_207352	M2	c.G1199A	p.R400H	comhet	0.000199681	0.00004118	D	D	D	[22]	
RP011	AR	RPI	NM_006269	M1	c.6179delA	p.E2060fs*12	hom	None	<0.000001	NA	NA	NA	[23]	
	AD	RPI	NM_006269	M1	c.C2029T	p.R677*	het	None	None	NA	NA	NA	[24]	
RP025	AD	RHO	NM_000539	M1	c.C403T	p.R135W	het	None	None	D	D	D	[25]	
RP038	AD	RHO	NM_000539	M1	c.C1040T	p.P347L	het	None	0.000008263	D	D	D	[26]	
RP014	AD	PRPF31	NM_015629	M1	c.967_968delGA	E323Dfs*151	het	None	None	NA	NA	NA	N ^o t reported	
RP019	AD	PRPF31	NM_015629	M1	c.327_330delCATC	p.H111Sfs*86	het	None	None	NA	NA	NA	N ^o t reported	
RP005	AD	PRPF3	NM_004698	M1	c.C1481T	p.T494M	het	None	None	D	D	D	[27]	
RP010	XLR	RP2	NM_006915	M1	c.758_761delTAAT	p.L253fs*10	hemi	None	None	NA	NA	NA	N ^o t reported	
RP012	AD	TOPORS	NM_001195622	M1	c.2323_2324delAG	p.S775*	het	None	None	NA	NA	NA	N ^o t reported	
RP018	AR	EYS	NM_001142800	M1	c.7228+1G>A	mis-splicing	comhet	None	None	NA	NA	NA	[28]	
	AR	EYS	NM_001142800	M2	c.4957dupA	p.S1653Kfs*2	comhet	None	None	NA	NA	NA	[29]	
RP027	AR	CNGAI	NM_001142564	M1	c.472delC	p.L89Ffs*4	hom	None	0.00009129	NA	NA	NA	[30]	

Family No.	Inheritance Model	Gene	NM No.	Mutation No.	Nucleotide change	Amino acid change	Frequencies			Software predictions			Reference	
							1000G	ExAC	SIFT	Poly-Phen	PRO-VEAN	1000G		ExAC
RP035	AR	<i>CNGBI</i>	NM_001297	M1	c.G2006A	p.W669*	None	None	None	NA	NA	NA	NA	N o t reported
RP036	XLR	<i>RPGR</i>	NM_000328	M1	c.T773C	p.L258P	None	None	None	D	D	D	D	N o t reported

Mutations not reported were bolded in the table. AR, autosomal recessive; AD, autosomal dominant; XLR, X-linked recessive; comhet, compound heterozygous; het, heterozygous; hom, homozygous; hemi, hemizygous; NA, not applicable; D, damaging.

TABLE 2. CLINICAL CHARACTERISTICS OF THE PATIENTS WHO VISITED OUTPATIENT DEPARTMENT IN 20 RP FAMILIES.

Family No.	Patient No.	Genotype	Gender	Disease Onset		Age	VA dec reased	BCVA OD	BCVA OS	IOP OD	IOP OS	Fundus Appearance		ERG OU	Humphrey preserved visual field_OD	Humphrey preserved visual field_OS	Complications
				se Onset	Age							OD	OS				
RP008	II:3	M1/M2	Male	15	NB	53	34	0.4	0.3	12	11	ARA,PBSL	NA	NA	NA	None	
RP015	II:1	M1/M2	Female	15	NB	44	-	0.7	0.7	11	12	Slight PBSL, ARA,ONP	NA	7.5	10	None	
RP028	II:4	M1/M2	Male	15	NB	57	40	LP	0.3	18	16	PBSL,ARA, ONP	D	Fail to complete	Fail to complete	Hearing loss	
RP033	II:5	M1/M2	Male	12	NB	51	40	HM	HM	14	14	PBSL,ARA, ONP	D	5	5	Early Cataract OU, hearing loss	
RP026	II:3	M1/M2	Female	20	NB	40	38	0.6	0.1	12.7	13	RF,profound atrophy	Rod D, cone dec reased	Temporal island	Temporal island	None	
RP034	II:2	M1/M2	Male	28	NB	55	40	HM	HM	11	12	PBSL, proufound atrophy, slight RF	D	Fail to complete	Fail to complete	None	
RP037	II:4	M1/M2	Male	32	NB	43	40	0.05	0.05	11	12	proufound RPE atrophy, slight RF	D	Superotemporal island	Superotemporal island	None	
				38	PV	52	45	HM	0.7	14	13	RPE atrophy,PBSL, ARA,ONP	D	Superotemporal island	Superotemporal island	None	

Family No.	Variants	Patient No.	Geno-type	Gen der	Age	Disease Onset		BCVA OD	BCVA OS	IOP OD	IOP OS	Fundus Appearance OD	ERG OU	Humphrey preserved visual field_OD	Humphrey preserved visual field_OS	Complications	
						Age	tom										
		II:5	M1/M2	Female	47	34	NB	39	HM	0.1	15	16	RPE atrophy,PBSL, ARA,ONP	D	Temporal island	Nasal island	None
RP011	RP1	II:2	M1/M1	Male	53	3	PV	30	FC/1m	FC/1m	14	15	slight pigments, profound RPE atrophy, ARA,ONP	D	Fail to complete	Fail to complete	OD post-surgical chronic cerebral circulation insufficiency
RP023	RP1	III:3	M1/+	Female	52	20	NB	25	0.4	0.6	9	12	slight pigments, profound RPE atrophy,ARA,ONP	D	5	5	None
RP025	RHO	I:1	M1/+	Female	39	EC	NB	13	LP	HM	18	17	Can't be seen	D	Fail to complete	Fail to complete	OU early-onset cataract
RP038	RHO	II:4	M1/+	Male	64	EC	NB	40	LP	LP	NA	NA	PBSL,ARA,ONP	NA	NA	NA	NA
		III:1	M1/+	Male	38	EC	NB	35	1	0.3	14	18	Slight PBSL, ARA,ONP	D	12.5	12.5	OU shallow anterior chamber
RP014	PRPF31	II:2	M1/+	Male	50	EC	NB	30	0.5	0.5	11	11	PBSL,ARA,ONP .posterior RPE atrophy,ERM	D	10	10	OU ERN

Family No.	Variants	Patient No.	Geno-type	Gen der	Age	Disease Onset		VA dec reased	BCVA OD	BCVA OS	IOP OD	IOP OS	Fundus Appearance		ERG OU	Humphrey preserved visual field_OD	Humphrey preserved visual field_OS	Complications
						Age	Age						OD	OS				
		III:1	M1/+	Male	16	EC	NB	-	0.8	0.8	14	15	15	slight pigments, posterior RPE atrophy	D	15	15	None
RP019	PRPF31	III:7	M1/+	Female	48	EC	NB	35	0.01	0.1	10	12	7.5	PBSL,ARA,ONP	D	Fail to complete	5	None
		III:1	M1/+	Female	68	EC	NB	56	LP	LP	9	11	Fail to complete	PBSL,ARA,ONP	D	Fail to complete	None	Traumatic optic nerve injury (OU)
RP005	PRPF3	II:2	M1/+	Male	62		NB	40	NLP	NLP	16	40	Fail to complete	ARA,PBSL,ONP	D	Fail to complete	1996 OS glaucoma since 2012; OS atresia iridis	
		IV:4	M1/+	Female	10		NB	-	1	1	14.8	13	Normal			periphera decreased to 15dB	periphera decreased to 15dB	None
RP010	RP2	III:2	M1	Male	18	EC	NB	NA	0.1	0.1	20.8	21	NA	slight PBSL,ARA	NA	NA	NA	None
RP012	TOPORS	V:1	M1/+	Female	22		NB	-	1	1	15	14	24	PBSL,ARA,ONP	NA	NA	20	NA
RP018	EYS	II:1	M1/M2	Female	37		NB	29	0.1	0.1	13	12	10	PBSL,ARA,ONP	D	10	5	None
		II:2	M1/M2	Male	35		NB	29	0.1	0.1	10	10	7.5	PBSL,ARA	D	7.5	0	None
RP027	CNGAI	II:1	M1/M1	Female	40	EC	NB	20	0.02	0.02	NA	NA	NA	PBSL,ARA,ONP	NA	NA	NA	None

Family No.	Variants	Patient No.	Geno-type	Gen-der	Disease Onset		VA dec reased Age	BCVA		IOP		Fundus Appearance		ERG		Humphrey preserved visual field		Humphrey preserved visual field_OS	Compi-cations
					Age	EC		OS	OD	OS	OD	OS	OD	OU	OD	OS			
		II:2	M1/M1	Male	39	EC	20	0.2	0.2	11	10	PBSL,ARA,ONP	D	10	10	10	None		
RP035	CNGBI	II:5	M1/M1	Male	64	5 NB	25	0.6 FC	16	11	ARA, ONP,profound RPE atrophy	D	5	5	5	None			
RP036	RPGR	III:2	M1	Male	49	EC	40	0.3	0.3	9	9	PBSL,ARA,ONP	D	10	10	None			
		III:5	M1	Male	48	EC	35 FC	FC	20	12	PBSL,ARA,ONP	D	15	20	20	None			
		IV:2	M1/+	Female	30	EC	NB	0.2	0.3	15	14	Leopard fundus,slight AR,posterior RPE atrophy	D	10	10	High myopia OD - HD OS - HD			

HM, hand move; FC, Finger count; LP, light perception; NLP, no light perception; EC, early childhood which was defined as before 5; ARA, attenuated retinal arteries; ONP, optic nerve pale; PBSL, pigment bone spicule-like; RF, refractile crystals in fundus; RPE, retinal pigmental epithelium; D, diminished; NA, not applicable

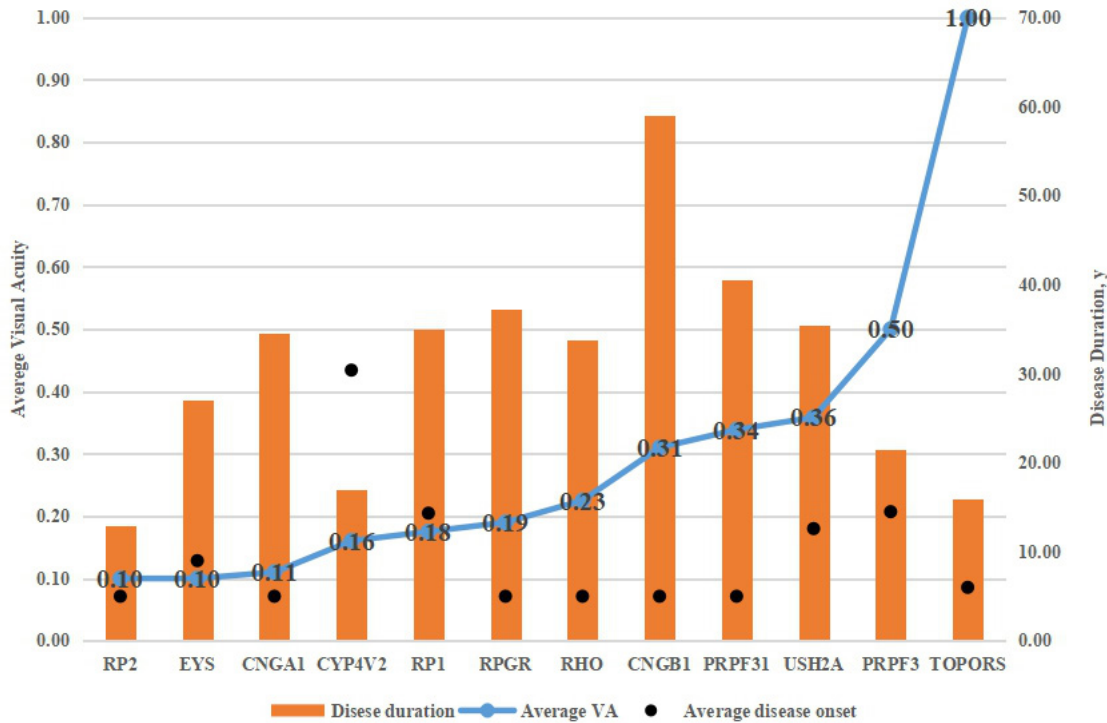


Figure 2. Phenotype–genotype relationship. Bars represent average disease duration of each gene; blue line and annotated data aside represent average visual acuity of individuals in each gene; black dots represent average disease onset in each gene.

department showed a defect in the fundus with mild to moderate peripheral bone spicule-like pigments, gray retina color, and attenuation of retinal vessels (Figure 3). Patients in family RP008 and family RP028 had hearing defects, so we revisited and rediagnosed the patients in RP008 and RP028 as having Usher syndrome type II. The other two families, RP015 and RP033, did not have obvious hearing problems; they were diagnosed as having simple RP.

CYP4V2 accounted for 15% (3/20) of mutations detected in this research. All three families with *CYP4V2* mutation (RP026, RP034, RP037) showed a compound heterozygous mutation pattern, and the patients in these three families were revisited and rediagnosed as having BCD. Five mutations identified in this research had been reported previously. In the three families, all six patients (five visited our outpatient department and one provided medical materials from a local hospital) showed highly reflective crystal deposits and profound RPE atrophy in the fundus photography (Figure 4). Five patients who could complete the visual field test all showed acentric visual field islands.

RPI, *RHO*, and *PRPF31* each accounted for two (2/20, 10%) families in this research. *TOPORS*, *EYS*, *CNGA1*, *CNGB1*, and *RPGR* were all identified in only one (1/20, 5%)

family. All clinical data for these patients are listed in Table 2, and fundus images are shown in Appendix 3. Novel mutations in these families are elaborated on below.

One novel mutation in *PRPF31* was identified as pathogenic in family RP014—namely, c.967_968delGA(E323Dfs*151). This novel mutation was a small deletion mutation, which led to translation frameshift and protein truncation. This may cause abnormal posttranslation after 323 amino acids, potentially leading to the abnormal function of the C-terminal domain and affecting the normal localization of protein in cells [32]. The mutation was identified as pathogenic according to the analysis of the ACMG guidelines. Two patients in RP014 showed moderate visual defect, with slight pigments in the fundus (Figure 5).

One novel mutation in *RP2* was identified as pathogenic in family RP010—namely, c.758_761delTAAT (p.I253fs*10). This was a small deletion mutation and led to translation frameshift and protein truncation. The C-terminal domain of the RP2 (RP2 activator of ARL3 GTPase) protein has weak homology with nucleoside diphosphate kinase (NDK). The mutation causing protein truncation has been reported to relate to a more severe phenotype [33]. Moreover, Jayasundera et al. reported that two different missense mutations at amino

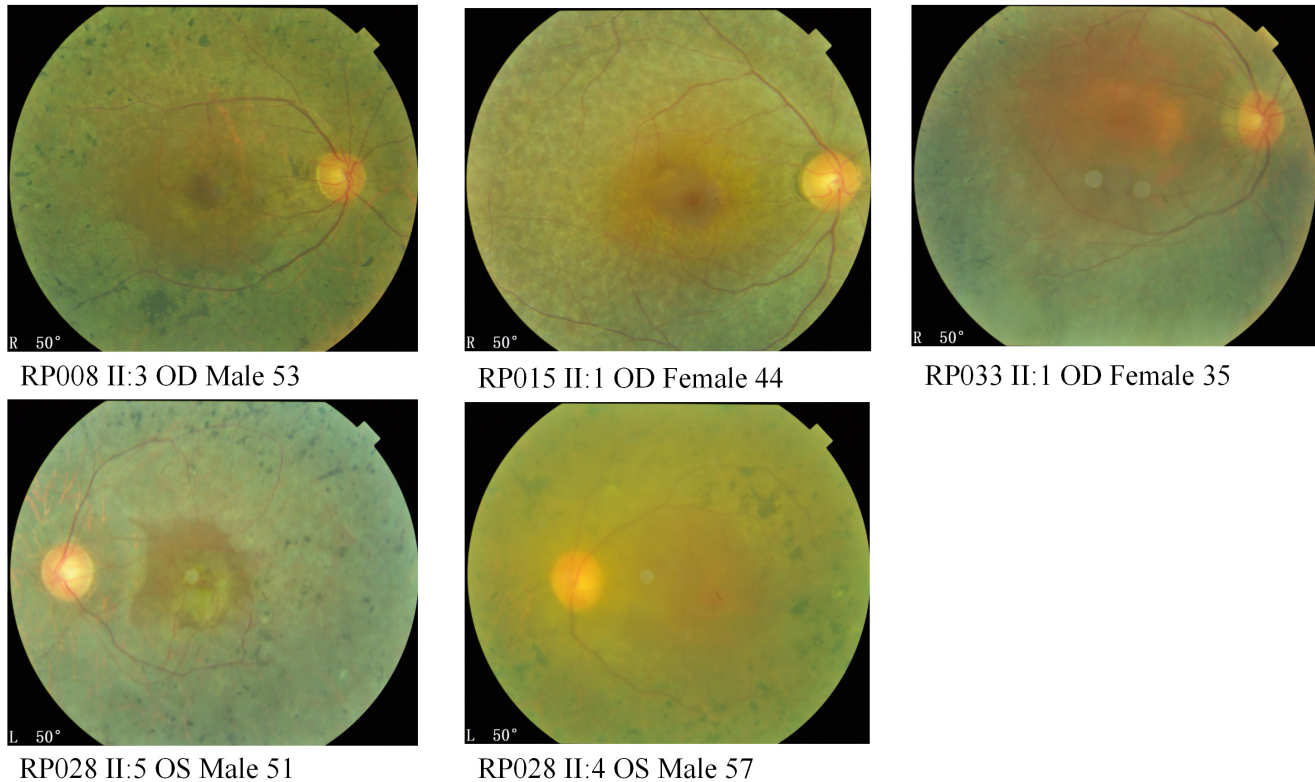


Figure 3. Fundus images of patients with *USH2A* mutations.

acid 253 lead to more severe phenotypes in *RP2* mutations [34]. In family RP010, the fundus of proband III:2 showed slight pigments and myopia in both eyes (oculus dexter [OD]: -5D, oculus sinister [OS]: -3.5D; Figure 5). In contrast, II:3—the mother of the proband, who was a carrier of this mutation—had high myopia of -14.5D in her left eye. In addition, II:2—the uncle of the proband, who did not come to the outpatient department of our hospital for examination—was totally blind at the age of 40 years. The local data provided showed that there was no light perception in either eye, and leopard fundus and high myopia were present in both eyes.

One novel mutation in *TOPORS* was identified in a large four-generation autosomal dominant family, family RP012—namely, c.2323_2324delAG, p.S775*. This small deletion mutation led to a truncated protein of 775 amino acids, resulting in partial loss of the RS domain and loss of two proline, glutamic acid, serine, and threonine (PEST) domains in the *TOPORS* protein. The RS domain is a region rich in arginine and serine, which may affect pre-mRNA splicing, whereas PEST domains are five residues rich in PEST elements (proline, glutamic acid, serine, and threonine), which are usually the characteristics of fast degradation

protein. Loss of these crucial domains may severely affect protein function [35]. This novel mutation was identified as pathogenic according to the ACMG guidelines. Eight patients tested in RP012 carried this heterozygous mutation; they all complained about night blindness from 6 to 17 years old accompanied by constricted visual field in adult age. The proband V:I who visited our outpatient department was a 22-year-old female. She complained about night blindness from 6 years old. At presentation, she had preserved a BCVA of 1.0 in both eyes but had a constricted visual field less than 24° (Figure 5).

A truncated mutation c.G2006A (p.W669*) in *CNGBI* was first reported in this research. This mutation was located in exon 10 (amino acids 661–838), which damages all key domains in *CNGBI* protein, including the N-terminal glutamate rich domain (encoded by exons 1 to 16), transmembrane and pore domain (encoded by exons 21 to 26), cyclic nucleotide-binding domain (encoded by exons 29 to 31), and carboxyl terminal channel-like domain [36]. This mutation may also trigger nonsense-mediated decay and affect the normal function of protein. This novel mutation was identified as pathogenic according to the ACMG guidelines. Two

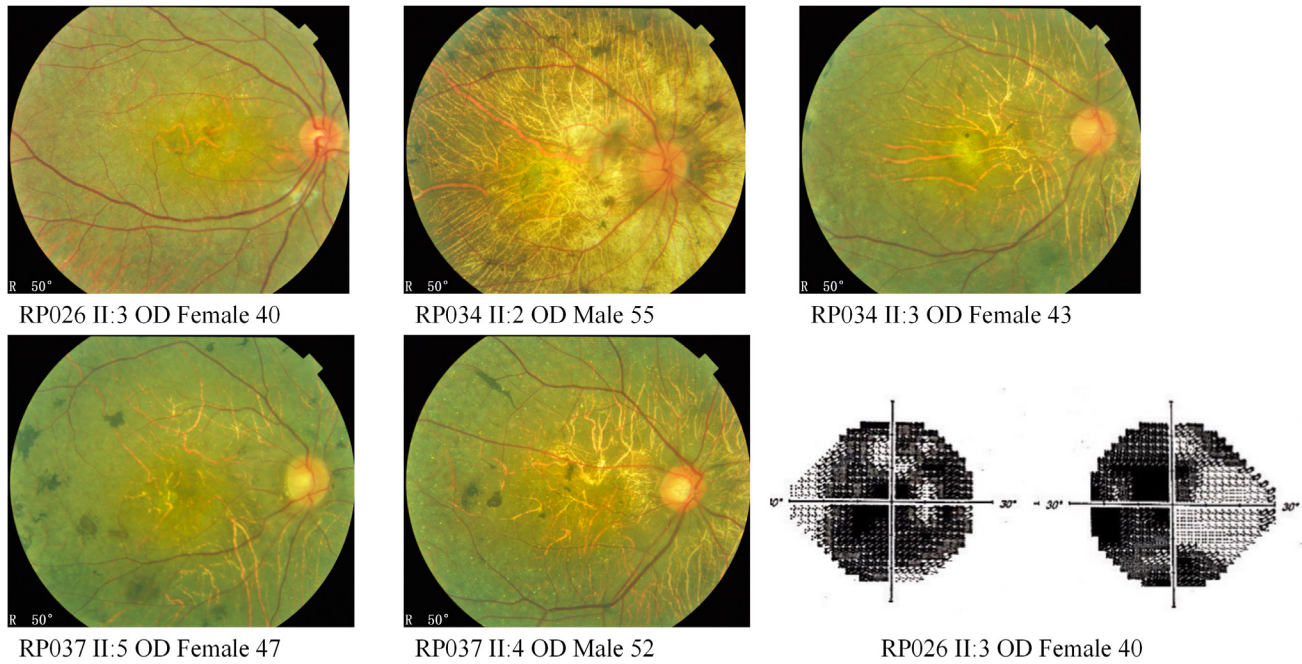


Figure 4. Fundus images of patients with *CYP4V2* mutations and typical acentric visual field from patient RP026 II:3.

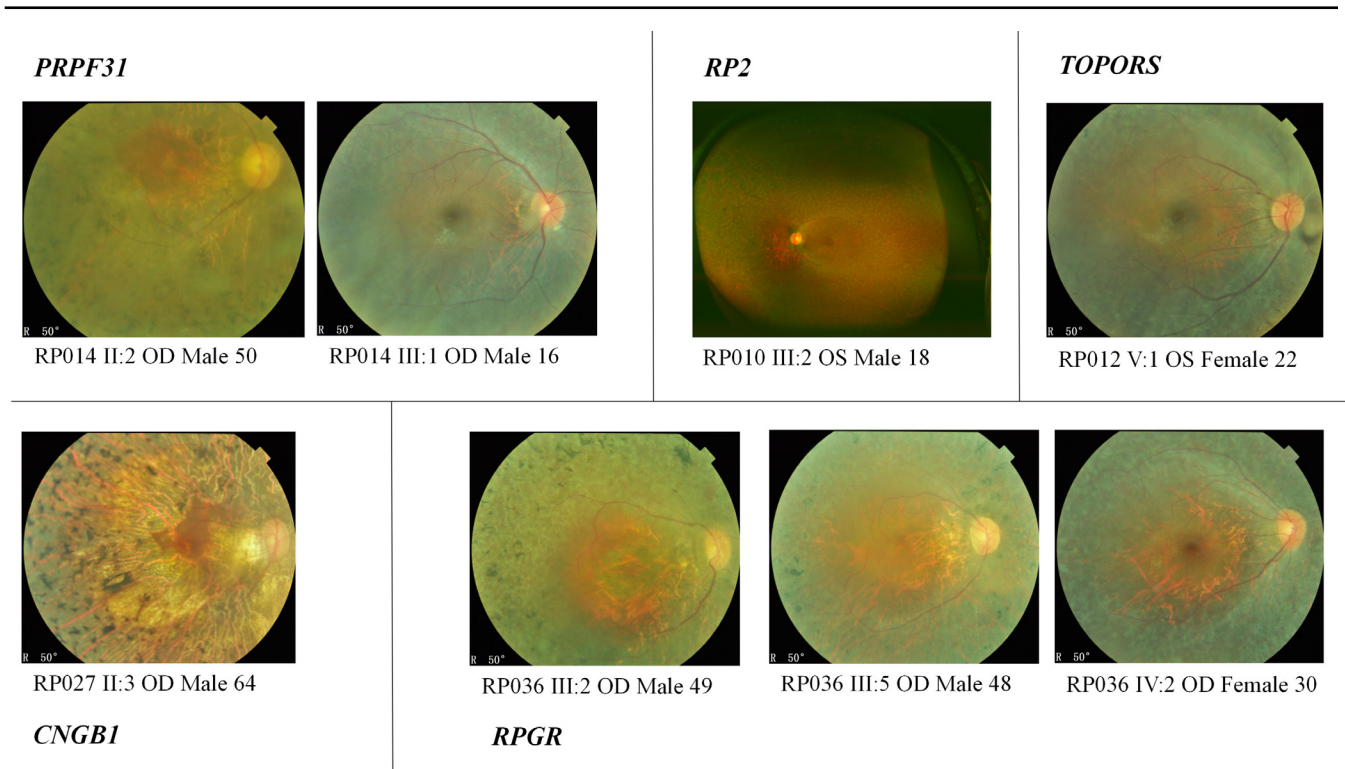


Figure 5. Fundus images of patients with novel mutations in *PRPF31*, *RP2*, *TOPORS*, *CNGBI*, and *RPGR*.

patients in family RP035 who carried this heterozygous mutation were siblings. Proband II:5 was a 64-year-old male, and his younger brother II:3 was 54 years old. They complained about night blindness before 5 years old and visual loss from the age of 25 (II:5) to their 40s (II:3). Dense pigments and profound RPE atrophy were found in the fundus of proband II:5 (Figure 5).

One novel mutation of *RPGR* (c.T773C, p.L258P), detected in the four-generation family RP036, was considered likely pathogenic. This missense mutation was located on exon 2 and was predicted to be damaging by PolyPhen, SIFT, and Provean. It has not been reported in the ExAC, 1000 Genomes, or Annoroad Healthy person mutation databases. According to ACMG guidelines, this novel mutation was identified as pathogenic. The proband III:5 and his three female cousins experienced night blindness from early childhood and visual defects from their 40s, whereas several female members of this family complained about high myopia over $-10.00D$. The female family member IV:2 had a high myopia of $-14.00D$ in the right eye and $-18.00D$ in the left eye. She had also complained about night blindness from early childhood, and her ERG examination showed diminished rod and cone responses. The fundus appearance of two patients showed dense pigments, attenuated retinal vessels, and a pale optic nerve head; in contrast, the fundus of the carrier female showed no pigments and a leopard fundus (Figure 5).

DISCUSSION

In this research, several important findings were reported, including the following: 1) 25 putative pathogenic mutations of 12 genes were detected by WES, and they were all confirmed by Sanger sequencing in 20 (20/28, 71.4%) families, including 12 genes with *USH2A* and *CYP4V2* as the most frequent mutated genes; 2) 7 novel mutations were identified, including *USH2A*, *PRPF31*, *RP2*, *TOPORS*, *CNGBI*, and *RPGR*; 3) the phenotype–genotype relationship in the 12 RP genes were analyzed which revealed later disease onset and more severe visual function defects in *CYP4V2*; and 4) late molecular diagnosis with long disease duration and poor preserved BCVA were found in Chinese RP patients.

Twelve genes were identified as putative pathogenic genes in this group of RP families, with *USH2A*, *CYP4V2*, *RHO*, *PRPF31*, and *RPI* as the most frequent genes. Several studies of the mutation spectrum in Chinese RP patients were reported previously, which were found to have some differences from our research (Table 3). *USH2A* (4/20, 20%) was detected to most frequently harbor the mutations in this research, which is consistent with the previously reported 12%–25% proportion worldwide [1,5]. *CYP4V2* (3/20, 15%)

was detected to be the second most frequent mutation gene in this research; *CYP4V2* encodes a member of the cytochrome P450 heme-thiolate protein superfamily, which is involved in oxidizing various substrates in the metabolic pathway. Mutations in this gene result in corneoretinal BCD [37]. This gene has been reported to account for 3% of RP patients in Caucasians [38]; it appears to be more common in East Asian countries, such as China [3] and Japan [39]. Recently, Gao et al. [40] reported a *CYP4V2* frequency of 15% in a large RD cohort comprising 1,243 patients, which indicated a large group of BCD patients in China. The differences in the most frequent mutation genes between this research and previous reports may come from study scales and different inclusion criteria because some studies may exclude BCD from RP. In addition, since BCD can be easily diagnosed from a unique fundus appearance, some clinicians may use Sanger sequencing as the detecting technology.

The diagnosis rate of WES sequencing in RDs varied greatly in previous studies because of the sequencing platform selection, inheritance pattern, and proband selection [11,12]. It has been reported that WES can achieve a diagnosis rate of 41%–55% [41–44] in large RP cohorts, and a higher diagnosis rate can be achieved in larger pedigrees. Panel-based NGS can promote a diagnosis rate of 70%–80% [40,45] in RDs by carefully designing the selected genes in the panel. When compared to WES, panel-based NGS was not applicable for small research groups because of the high cost of the panel design procedure. In this research, we achieved a diagnosis rate of 71.4%. There were three factors responsible for the relatively high diagnosis rate: First, probands recruited in this research all had a clear family history and clinical diagnosis. Second, at least one patient and one healthy relative were sent for WES sequencing. Third, mutations passed through the filtering procedure were searched from among 662 gene defects that can cause vision-associated phenotypes (including 89 RP genes in the RetNet Database). With the development of NGS, the cost of WES in each patient can be relatively low, making WES a more competitive approach for molecular diagnosis in RDs.

Seven novel mutations were detected in this study. All mutations were found to be cosegregated with phenotype, and they were confirmed by Sanger sequencing. Among the seven novel mutations, six were mutations causing protein truncation, which revealed that truncated mutations were still more common in RP molecular diagnosis.

Phenotype–genotype relationships were detected in this research. For the two most frequent genes in this research, *USH2A* was found to have a milder phenotype compared with *CYP4V2*, with longer disease duration and moderate

TABLE 3. LARGE COHORTS OF PREVIOUS STUDIES IN CHINESE IRDs.

Year	Author	Targeted Diseases	Sequencing Techniques	No. of Patients	Diagnosis Rate	Most Frequent Genes
2014	Xu Y and et al. [41]	RP	WES	157	79/157 (50%)	USH2A, RHO, RPGR, SNRNP200, PDE6B, RP2
2014	Huang XF and et al. [42]	RDs	Panel-based NGS	179	99/179 (55.3%)	USH2A, EYS, CRBL, PDE6B, ABCA4, CYP4V2
2017	Huang L and et al. [43]	RP	WES	98	40/98 (41%)	USH2A, RPI, RPGR, PRPF31, ABCA4
2019	Wu JH and et al. [40]	RP	Panel-based NGS	1243	896/1243 (72.8%)	USH2A, CYP4V2, EYS, RPGR, RHO, RPI

visual defect. Visual field tests in *CYP4V2* patients were also found to have a unique pattern, with preserved acentric visual field islands; this indicated that different strategies should be adopted in treating BCD from other sub types of RP.

Putative genes in eight families were not identified in this research. For RP031, *PRPF8* (c.C3543G, p.D1181E) has been identified as a putative gene; because the mutation and disease did not cosegregate, we excluded *PRPF8* as the putative mutation in RP031. There are several possible reasons that these mutations could not be found by WES, which are as follows [12]: 1) the mutations were larger deletions or rearrangements that are not detectable by WES; 2) the mutations were in deeper intronic mutations that cannot be detected by WES; and 3) the mutations were in genes that had not been reported to be associated with RP.

In conclusion, 25 putative pathogenic mutations of 12 genes were detected by WES and were all confirmed by Sanger sequencing in 20 (20/28, 71.4%) families, including 7 novel mutations. *USH2A* and *CYP4V2* were found to be the most frequent genes in this research. The mutation spectrum of RP in Chinese was expanded in this research, which may benefit future cutting-edge therapies.

APPENDIX 1. 89 RP GENES IN RETNET DATABASE.

To access the data, click or select the words “[Appendix 1.](#)”

APPENDIX 2. THE MAPPING RATE AND COVERAGE OF TARGETED REGION OF EACH SAMPLE.

To access the data, click or select the words “[Appendix 2.](#)”

APPENDIX 3. MUTATION TYPE SPECTRUM OF EACH GENE IN 20 FAMILIES.

To access the data, click or select the words “[Appendix 3.](#)”

APPENDIX 4. ALL SUSPICIOUS MUTATIONS FOUND IN EACH FAMILY AND THE REASON WE CHOSE PUTATIVE MUTATIONS.

To access the data, click or select the words “[Appendix 4.](#)”

APPENDIX 5. PEDIGREE CHARTS, SANGER SEQUENCING RESULTS FOR EACH MUTATED GENES.

To access the data, click or select the words “[Appendix 5.](#)” Fundus images for mutations in RHO, RP1, CNGA1, EYS, PRPF3 which have been reported previously

ACKNOWLEDGMENTS

Funding: Supported by The Capital Health Research and Development of Special (2020–1-2052; WWB); Science & Technology Project of Beijing Municipal Science & Technology Commission (Z181100001818003; WWB); the Beijing Municipal Administration of Hospitals’ Ascent Plan (DFL20150201; WWB); Beijing Natural Science Foundation (7,204,245), Scientific Research Common Program of Beijing Municipal Commission of Education (KM202010025018; LY); Beijing Municipal Administration of Hospitals’ Youth Programme (QML20190202; LY); Beijing Dongcheng District Outstanding Talents Cultivating Plan (2018; LY) Authors’ contributions: Conceptualization: [Chang Shen, Yang Li]; Methodology: [Chang Shen, Bing You, Wen-Bin Wei]; Formal analysis and investigation: [Chang Shen, Bing You, Yu-Ning Chen]; Writing - original draft preparation: [Chang Shen]; Writing - review and editing: [Yang Li, Wei Li, Wen-Bin Wei]; Funding acquisition: [Yang Li, Wen-Bin Wei]; Resources: [Wei Li, Yang Li, Wen-Bin Wei]; Supervision: [Yang Li, Wei Li, Wen-Bin Wei]. Ethics approval: All procedures performed in studies involving human participants were in accordance with the ethical standards of the institutional and/or national research committee and with the 1964 Helsinki declaration and its later amendments or comparable ethical standards. The study was approved by the Medical Ethics Committee of the Beijing Tongren Hospital, and written informed consent was obtained from all study participants, and all methods were performed in accordance with the relevant guidelines and regulations. Dr. Yang Li (liyong_8151@126.com), Dr. Wei Li (liweili@ioz.ac.cn) and Dr. Wen-Bin Wei (weibenbin@163.com) are co-corresponding authors for this paper.

REFERENCES

- Hartong DT, Berson EL, Dryja TP. Retinitis pigmentosa. *Lancet* 2006; 368:1795-809. [PMID: 17113430].
- You QS, Xu L, Wang YX, Liang QF, Cui TT, Yang XH, Wang S, Yang H, Jonas JB. Prevalence of retinitis pigmentosa in North China: the Beijing Eye Public Health Care Project. *Acta Ophthalmol* 2013; 91:e499-500. [PMID: 23764135].
- Hu DN. Prevalence and mode of inheritance of major genetic eye diseases in China. *J Med Genet* 1987; 24:584-8. [PMID: 3500313].
- Xu L, Hu L, Ma K, Li J, Jonas JB. Prevalence of retinitis pigmentosa in urban and rural adult Chinese: The Beijing Eye Study. *Eur J Ophthalmol* 2006; 16:865-6. [PMID: 17191195].
- Verbakel SK, van Huet R, Boon C, den Hollander AI, Collin R, Klaver C, Hoyng CB, Roepman R, Klevering BJ. Non-syndromic retinitis pigmentosa. *Prog Retin Eye Res* 2018; 66:157-86. [PMID: 29597005].

6. Dias MF, Joo K, Kemp JA, Fialho SL, Da SCAJ, Woo SJ, Kwon YJ. Molecular genetics and emerging therapies for retinitis pigmentosa: Basic research and clinical perspectives. *Prog Retin Eye Res* 2018; 63:107-31. [PMID: 29097191].
7. Russell S, Bennett J, Wellman JA, Chung DC, Yu ZF, Tillman A, Wittes J, Pappas J, Elci O, McCague S, Cross D, Marshall KA, Walshire J, Kehoe TL, Reichert H, Davis M, Raffini L, George LA, Hudson FP, Dingfield L, Zhu X, Haller JA, Sohn EH, Mahajan VB, Pfeifer W, Weckmann M, Johnson C, Gewaily D, Drack A, Stone E, Wachtel K, Simonelli F, Leroy BP, Wright JF, High KA, Maguire AM. Efficacy and safety of voretigene neparvovec (AAV2-hRPE65v2) in patients with RPE65-mediated inherited retinal dystrophy: a randomised, controlled, open-label, phase 3 trial. *Lancet* 2017; 390:849-60. [PMID: 28712537].
8. Ghazi NG, Abboud EB, Nowilaty SR, Alkuraya H, Alhom-madi A, Cai H, Hou R, Deng WT, Boye SL, Almaghami A, Al SF, Al-Dhibi H, Birch D, Chung C, Colak D, LaVail MM, Vollrath D, Erger K, Wang W, Conlon T, Zhang K, Hauswirth W, Alkuraya FS. Treatment of retinitis pigmentosa due to MERTK mutations by ocular subretinal injection of adeno-associated virus gene vector: results of a phase I trial. *Hum Genet* 2016; 135:327-43. [PMID: 26825853].
9. Xue K, MacLaren RE. Ocular gene therapy for choroideremia: clinical trials and future perspectives. *Expert Rev Ophthalmol* 2018; 13:129-38. [PMID: 31105764].
10. Chacon-Camacho OF, Garcia-Montano LA, Zenteno JC. The clinical implications of molecular monitoring and analyses of inherited retinal diseases. *Expert Rev Mol Diagn* 2017; 17:1009-21. [PMID: 28945154].
11. Chaitankar V, Karakulah G, Ratnapriya R, Giuste FO, Brooks MJ, Swaroop A. Next generation sequencing technology and genomewide data analysis: Perspectives for retinal research. *Prog Retin Eye Res* 2016; 55:1-31. [PMID: 27297499].
12. Gilissen C, Hoischen A, Brunner HG, Veltman JA. Disease gene identification strategies for exome sequencing. *Eur J Hum Genet* 2012; 20:490-7. [PMID: 22258526].
13. Kumar P, Henikoff S, Ng PC. Predicting the effects of coding non-synonymous variants on protein function using the SIFT algorithm. *Nat Protoc* 2009; 4:1073-81. [PMID: 19561590].
14. Adzhubei IA, Schmidt S, Peshkin L, Ramensky VE, Gerasimova A, Bork P, Kondrashov AS, Sunyaev SR. A method and server for predicting damaging missense mutations. *Nat Methods* 2010; 7:248-9. [PMID: 20354512].
15. Richards S, Aziz N, Bale S, Bick D, Das S, Gastier-Foster J, Grody WW, Hegde M, Lyon E, Spector E, Voelkerding K, Rehm HL. Standards and guidelines for the interpretation of sequence variants: a joint consensus recommendation of the American College of Medical Genetics and Genomics and the Association for Molecular Pathology. *Genet Med* 2015; 17:405-24. [PMID: 25741868].
16. Weston MD, Eudy JD, Fujita S, Yao S, Usami S, Cremers C, Greenberg J, Ramesar R, Martini A, Moller C, Smith RJ, Sumegi J, Kimberling WJ. Genomic structure and identification of novel mutations in usherin, the gene responsible for Usher syndrome type IIa. *Am J Hum Genet* 2000; 66:1199-210. [PMID: 10729113].
17. Chen X, Sheng X, Liu X, Li H, Liu Y, Rong W, Ha S, Liu W, Kang X, Zhao K, Zhao C. Targeted next-generation sequencing reveals novel USH2A mutations associated with diverse disease phenotypes: implications for clinical and molecular diagnosis. *PLoS One* 2014; 9:e105439-[PMID: 25133613].
18. Xu W, Dai H, Lu T, Zhang X, Dong B, Li Y. Seven novel mutations in the long isoform of the USH2A gene in Chinese families with nonsyndromic retinitis pigmentosa and Usher syndrome Type II. *Mol Vis* 2011; 17:1537-52. [PMID: 21686329].
19. Yin H, Jin C, Fang X, Miao Q, Zhao Y, Chen Z, Su Z, Ye P, Wang Y, Yin J. Molecular analysis and phenotypic study in 14 Chinese families with Bietti crystalline dystrophy. *PLoS One* 2014; 9:e94960-[PMID: 24739949].
20. Xiao X, Mai G, Li S, Guo X, Zhang Q. Identification of CYP4V2 mutation in 21 families and overview of mutation spectrum in Bietti crystalline corneoretinal dystrophy. *Biochem Biophys Res Commun* 2011; 409:181-6. [PMID: 21565171].
21. Li A, Jiao X, Munier FL, Schorderet DF, Yao W, Iwata F, Hayakawa M, Kanai A, Shy CM, Alan LR, Heckenlively J, Weleber RG, Traboulsi EI, Zhang Q, Xiao X, Kaiser-Kupfer M, Sergeev YV, Hejtmancik JF. Bietti crystalline corneoretinal dystrophy is caused by mutations in the novel gene CYP4V2. *Am J Hum Genet* 2004; 74:817-26. [PMID: 15042513].
22. Vargas M, Mitchell A, Yang P, Weleber R. Bietti Crystalline Dystrophy. *Gene Reviews*. 1993.
23. Li S, Yang M, Liu W, Liu Y, Zhang L, Yang Y, Sundaresan P, Yang Z, Zhu X. Targeted Next-Generation Sequencing Reveals Novel RP1 Mutations in Autosomal Recessive Retinitis Pigmentosa. *Genet Test Mol Biomarkers* 2018; 22:109-14. [PMID: 29425069].
24. Blanton SH, Heckenlively JR, Cottingham AW, Friedman J, Sadler LA, Wagner M, Friedman LH, Daiger SP. Linkage mapping of autosomal dominant retinitis pigmentosa (RP1) to the pericentric region of human chromosome 8. *Genomics* 1991; 11:857-69. [PMID: 1783394].
25. Al-Magtheth M, Gregory C, Inglehearn C, Hardcastle A, Bhattacharya S. Rhodopsin mutations in autosomal dominant retinitis pigmentosa. *Hum Mutat* 1993; 2:249-55. [PMID: 8401533].
26. Dryja TP, McGee TL, Hahn LB, Cowley GS, Olsson JE, Reichel E, Sandberg MA, Berson EL. Mutations within the rhodopsin gene in patients with autosomal dominant retinitis pigmentosa. *N Engl J Med* 1990; 323:1302-7. [PMID: 2215617].
27. Chakarova CF, Hims MM, Bolz H, Abu-Safieh L, Patel RJ, Papaioannou MG, Inglehearn CF, Keen TJ, Willis C, Moore AT, Rosenberg T, Webster AR, Bird AC, Gal A, Hunt D, Vithana EN, Bhattacharya SS. Mutations in HPRP3, a third member of pre-mRNA splicing factor genes, implicated in

- autosomal dominant retinitis pigmentosa. *Hum Mol Genet* 2002; 11:87-92. [PMID: 11773002].
28. Messchaert M, Haer-Wigman L, Khan MI, Cremers F, Collin R. EYS mutation update: In silico assessment of 271 reported and 26 novel variants in patients with retinitis pigmentosa. *Hum Mutat* 2018; 39:177-86. [PMID: 29159838].
 29. Hosono K, Ishigami C, Takahashi M, Park DH, Hirami Y, Nakanishi H, Ueno S, Yokoi T, Hikoya A, Fujita T, Zhao Y, Nishina S, Shin JP, Kim IT, Yamamoto S, Azuma N, Terasaki H, Sato M, Kondo M, Minoshima S, Hotta Y. Two novel mutations in the EYS gene are possible major causes of autosomal recessive retinitis pigmentosa in the Japanese population. *PLoS One* 2012; 7:e31036-[PMID: 22363543].
 30. Dryja TP, Finn JT, Peng YW, McGee TL, Berson EL, Yau KW. Mutations in the gene encoding the alpha subunit of the rod cGMP-gated channel in autosomal recessive retinitis pigmentosa. *Proc Natl Acad Sci USA* 1995; 92:10177-81. [PMID: 7479749].
 31. van Wijk E, Pennings RJ, Te BH, Claassen A, Yntema HG, Hoefsloot LH, Cremers FP, Cremers CW, Kremer H. Identification of 51 novel exons of the Usher syndrome type 2A (USH2A) gene that encode multiple conserved functional domains and that are mutated in patients with Usher syndrome type II. *Am J Hum Genet* 2004; 74:738-44. [PMID: 15015129].
 32. Wang J, Gui L, Chen ZY, Zhang QY. Mutations in the C-terminal region affect subcellular localization of crucian carp herpesvirus (CaHV) GPCR. *Virus Genes* 2016; 52:484-94. [PMID: 27059239].
 33. Lyraki R, Megaw R, Hurd T. Disease mechanisms of X-linked retinitis pigmentosa due to RP2 and RPGR mutations. *Biochem Soc Trans* 2016; 44:1235-44. [PMID: 27911705].
 34. Jayasundera T, Branham KE, Othman M, Rhoades WR, Karoukis AJ, Khanna H, Swaroop A, Heckenlively JR. RP2 phenotype and pathogenetic correlations in X-linked retinitis pigmentosa. *Arch Ophthalmol* 2010; 128:915-23. [PMID: 20625056].
 35. Selmer KK, Grondahl J, Riise R, Brandal K, Braaten O, Bragadottir R, Undlien DE. Autosomal dominant pericentral retinal dystrophy caused by a novel missense mutation in the TOPORS gene. *Acta Ophthalmol* 2010; 88:323-8. [PMID: 19183411].
 36. Ardell MD, Bedsole DL, Schoborg RV, Pittler SJ. Genomic organization of the human rod photoreceptor cGMP-gated cation channel beta-subunit gene. *Gene* 2000; 245:311-8. [PMID: 10717482].
 37. Li A, Jiao X, Munier FL, Schorderet DF, Yao W, Iwata F, Hayakawa M, Kanai A, Shy CM, Alan LR, Heckenlively J, Weleber RG, Traboulsi EI, Zhang Q, Xiao X, Kaiser-Kupfer M, Sergeev YV, Hejtmancik JF. Bietti crystalline corneoretinal dystrophy is caused by mutations in the novel gene CYP4V2. *Am J Hum Genet* 2004; 74:817-26. [PMID: 15042513].
 38. Mataftsi A, Zografos L, Milla E, Secretan M, Munier FL. Bietti's crystalline corneoretinal dystrophy: a cross-sectional study. *Retina* 2004; 24:416-26. [PMID: 15187665].
 39. Lin J, Nishiguchi KM, Nakamura M, Dryja TP, Berson EL, Miyake Y. Recessive mutations in the CYP4V2 gene in East Asian and Middle Eastern patients with Bietti crystalline corneoretinal dystrophy. *J Med Genet* 2005; 42:e38-[PMID: 15937078].
 40. Gao FJ, Li JK, Chen H, Hu FY, Zhang SH, Qi YH, Xu P, Wang DD, Wang LS, Chang Q, Zhang YJ, Liu W, Li W, Wang M, Chen F, Xu GZ, Wu JH. Genetic and Clinical Findings in a Large Cohort of Chinese Patients with Suspected Retinitis Pigmentosa. *Ophthalmology* 2019; 126:1549-56. [PMID: 31054281].
 41. Xu Y, Guan L, Shen T, Zhang J, Xiao X, Jiang H, Li S, Yang J, Jia X, Yin Y, Guo X, Wang J, Zhang Q. Mutations of 60 known causative genes in 157 families with retinitis pigmentosa based on exome sequencing. *Hum Genet* 2014; 133:1255-71. [PMID: 24938718].
 42. Huang XF, Huang F, Wu KC, Wu J, Chen J, Pang CP, Lu F, Qu J, Jin ZB. Genotype-phenotype correlation and mutation spectrum in a large cohort of patients with inherited retinal dystrophy revealed by next-generation sequencing. *Genet Med* 2015; 17:271-8. [PMID: 25356976].
 43. Huang L, Zhang Q, Huang X, Qu C, Ma S, Mao Y, Yang J, Li Y, Li Y, Tan C, Zhao P, Yang Z. Mutation screening in genes known to be responsible for Retinitis Pigmentosa in 98 Small Han Chinese Families. *Sci Rep* 2017; 7:1948-59. [PMID: 28512305].
 44. Xu Y, Guan L, Xiao X, Zhang J, Li S, Jiang H, Jia X, Yang J, Guo X, Yin Y, Wang J, Zhang Q. Mutation analysis in 129 genes associated with other forms of retinal dystrophy in 157 families with retinitis pigmentosa based on exome sequencing. *Mol Vis* 2015; 21:477-86. [PMID: 25999675].
 45. Taylor RL, Parry N, Barton SJ, Campbell C, Delaney CM, Ellingford JM. Panel-Based Clinical Genetic Testing in 85 Children with Inherited Retinal Disease. *Ophthalmology* 2017; 124:985-91. [PMID: 28341476].

Articles are provided courtesy of Emory University and the Zhongshan Ophthalmic Center, Sun Yat-sen University, P.R. China. The print version of this article was created on 6 June 2022. This reflects all typographical corrections and errata to the article through that date. Details of any changes may be found in the online version of the article.